

HC1569 - Time-resolved imaging of phase-locked vortex precession

Scientific motivations

From previous studies on pairs of oscillators it is known that a synchronised ('phase-locked') precession of two oscillators can be achieved via the dipolar coupling interaction associated with the direction of the moments in the neighbouring vortex structures. In this experiment we proposed to explore the phase locking mechanism of periodically structured arrays of oscillators. To understand the dynamics of the of the vortices and their coupling effects we proposed to carry out time-resolved imaging using Holography with Extended Reference by Autocorrelation Linear Differential Operation (HERALDO).

In the initial stage of measurements the aim was to establish the time-resolved holographic imaging and demonstrate first results of observations of vortex core gyration in square Py elements which comprise a large periodic array.

Experimental Set-up

The experiments were carried out on the holographic imaging setup of ID-32 branch line. In order to undertake the stroboscopic imaging we used 16 bunch synchrotron filling pattern. Figure 1 shows the experimental setup together with the time structure of the magnetic 'pump' and the x-ray 'probe' pulses.

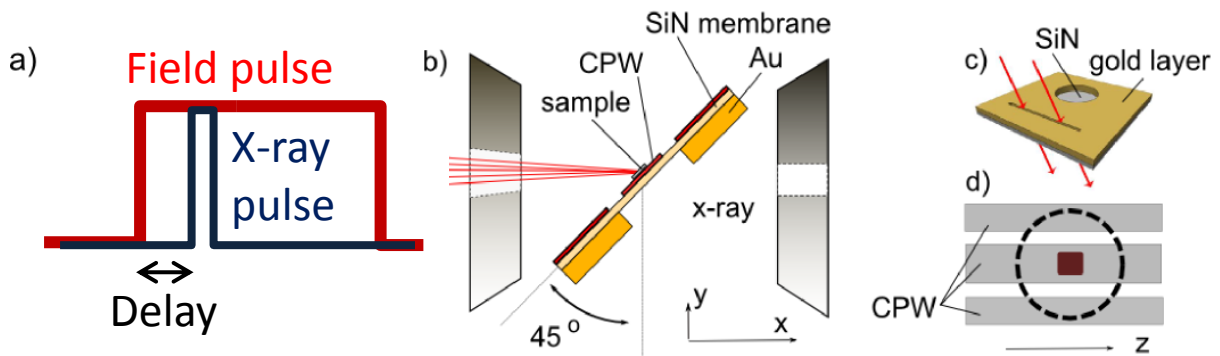


Fig. 1. Schematics of the experimental set-up. a) Stroboscopic imaging in pulsed excitation in 16 bunch mode. Magnetic pulse is triggered by x-ray bunch and is delayed by dt . b) Orientation of the sample with respect to the x-ray beam and the direction of the bias field supplied by the two magnet poles. c) Sample design. The front side of the SiN membrane (200 nm thick) is covered with 700 nm gold mask blocking the x-rays everywhere apart from the area of the circular aperture and the reference slit. The reference slit (20-40 nm) is in the incidence plane allowing x-ray go through. d) NiFe element and the coplanar waveguide (CPW) tracks on the other side of the membrane behind the aperture.

To apply the magnetic pulses the samples contained integrated coplanar waveguides (figure 1d) which was connected to an RF pulse generator via SMA coaxial cabling and the feedthroughs. The exact design of this network is critical for the measurements as it defines the amplitude of the magnetic field pulse. The latter determines the extent of the gyration (see figure 4). If the field is not sufficient the gyration radius can be too small to resolve the effect, or vice-versa, it can be too big for the gyration to be sustained. From the calculations, based on the maximum amplitude of the magnetic pulse (3.8V) and the width of the central track of the CPW (5 micron), the field obtained on the sample should be up to 70 Oe, which is

sufficient to produce gyration over 200 nm in radius. The real field however, is usually smaller, because of reflections. In particular, we have to use wire bonding to connect CPW to the SMA connector. The characteristic impedance of the wires are different to 50 Ohm, thus leading to reflected power. The extent of these losses however, cannot be easily measured, and can only be estimated from the imaging results. Based on our simulations and the amount of vortex core shift (figure 4), it is believed that the actual magnetic field from the CPW was not exceeding 20-30 Oe.

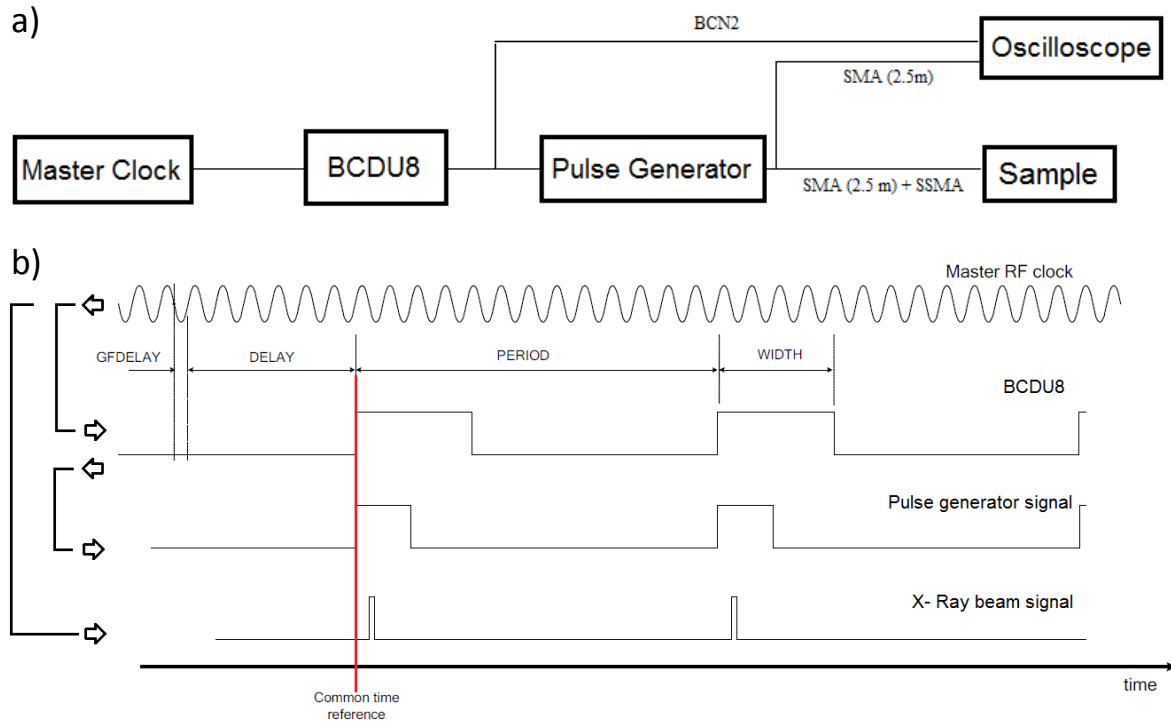


Fig. 2. Schematics of the set-up in time-resolved measurements: a) RF Connections, b) Time structure of the pump and the probe pulses.

The excitation of the gyration was achieved using a pulse structure shown in figure 2 b). The magnetic pulses were produced by a functional generator Agilent 8110A, which was synchronised with the synchrotron master clock. At ID32 we used BCDU8 unit that can generate pulses of different length, period and delay with respect to the synchrotron RF clock cycle. We used BCDU8 to trigger the functional generator and also for controlling the necessary delay between the ‘pump’ and ‘probe’ pulses. The length of the magnetic pulse (~60 ns) was chosen sufficiently long to sustain the core gyration cycles, the amplitude of which gets significantly dumped towards the end of each gyration (see figure 3). The dynamic band of the expected eigenmodes was defined by the rise time of the magnetic pulse ($f \approx 1/\tau_{rise}$). Agilent 8110A provides the minimum rise time 800 ps, which was used in the measurements. From the micromagnetic simulations, it is known that the frequency gyration modes are in direct relation to the aspect ratio of the elements thickness/width. To satisfy these requirements, the size of the elements have been chosen greater than 1000 nm, which should have gyration frequencies below 300 MHz. In order to account for the additional delays accumulated in the coaxial cables and all other RF components, we have used an avalanche diode to detect the exact timing of x-ray pulses arriving to the sample. The diode was placed instead of the sample in the beginning of the experiment, and then removed on the

assumption that the time structure of the x-rays should remain fixed for the duration of the beamtime.

The main sample used in the measurements consisted of a 50 nm thick, 2000 x 2000 nm Py magnetic film which was sputtered onto an x-ray transparent Si_3N_4 membrane, so that transmission measurements could be performed. On the reverse side of the membrane, an x-ray opaque Au mask was deposited, and FIB patterned with a 5 μm field of view (FOV) aperture, and near-by extended holographic reference slit (6 μm in length and 30 nm wide). The size and separation of the FOV aperture and extended reference slit were chosen such that when illuminated by the x-rays, they were within the beams coherent area. The diffraction chamber on ID32 was fitted with a CCD camera positioned behind the sample, which we used to record far-field diffraction patterns from light scattered by the Py disc within the FOV aperture, and holographic reference slit. The interference between the disc and the reference slit produces a hologram which can be easily reconstructed to form a real space image with magnetic contrast. The strength of the magnetic scattering signal is proportional to $\mathbf{M} \cdot \mathbf{k}_i$, i.e. the projection of the incident wave vector of light, \mathbf{k}_i , onto the magnetization \mathbf{M} of the sample. In order to produce a non-zero scattering signal from the in-plane magnetized domains in the Py square, we rotated the sample by 45 degrees within the x-ray beam. The orientation of the reference slit was chosen so that the direction along the length of the slit was perpendicular to the samples rotation axis. This enabled the x-rays to be transmitted through the slit, and not blocked by the Au mask, when the sample was placed in its rotated position [as demonstrated in Figure 1 (b)]. A magnet was positioned outside the ID32 diffraction chamber which could be used to apply an external magnetic field to our sample whilst images were being taken.

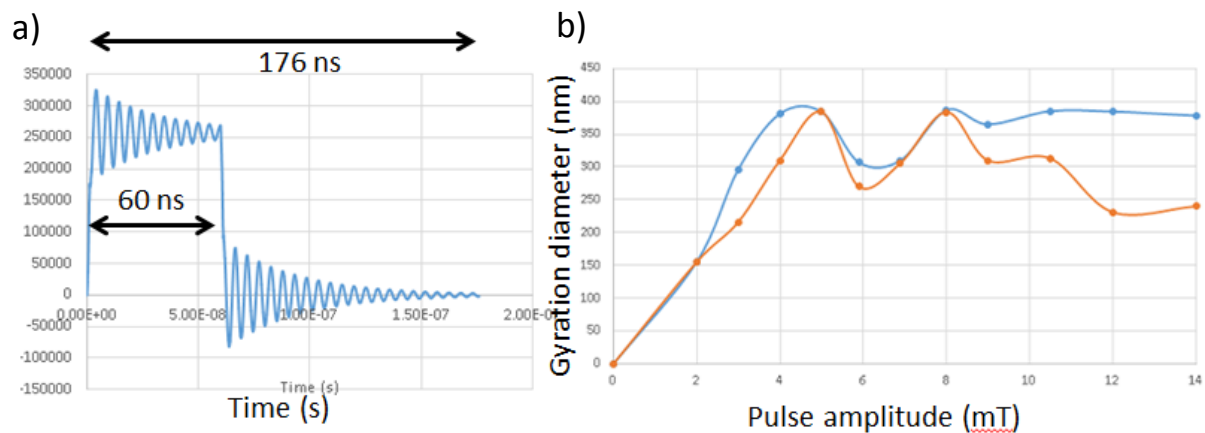


Fig. 3. Micromagnetic simulation of the vortex core gyration in a Py 2000x2000 nm square element . a) Average magnetisation (y-component) vs time of excitation. b) Gyration diameter vs pulse amplitude.

To guide the experimental work we used micromagnetic simulations performed by OOMMF. Figure 3 shows the results of this work, including the oscillation of the average magnetisation of the x-component a) and the dependence of the gyration diameter on the amplitude of the magnetic pulse b). It can be seen from the figure that once the gyration commences it is quickly dumped within the duration of the pulse. Given a non-zero magnetic field component the average value of magnetisation is also non-zero, and the position of the core is displaced from the centre along the 'y' (vertical) direction. At the trailing edge of the magnetic pulse the gyration is excited again, but now at the centre of the element. Towards the end of the 176 ns period the gyration is practically negligent, so when another cycle of gyration is commenced the track of the core repeats the previous track and the phases of gyration.

Results of the Experiment

Figure 4(a) shows a typical diffraction pattern recorded on the CCD, and figure 4(b) shows the reconstructed domain patterns at different delay times after the leading edge of the magnetic pulse. Figure 4(c) also shows the positions of the core at different delay times. The plotted line extrapolates the predicted track of the core based on these positions. Having analyzed the reconstructed images, it is clear that the core of the vortex has different positions at different delay times, indicating that the vortex is excited by the magnetic pulse and follows cyclic motion. The displacement can be seen in both horizontal and vertical directions. If a more detailed analysis is given it can be seen that not only the core is moving but the whole pattern is modified. In particular the domain walls of the closure are also modified. This is particularly clear if the images are seen in a movie sequence. From the simulations, it is well known that just after the excitation there is a number of high frequency modes that can be seen in such structures, but these are normally quickly dumped within the first several cycles of gyration.

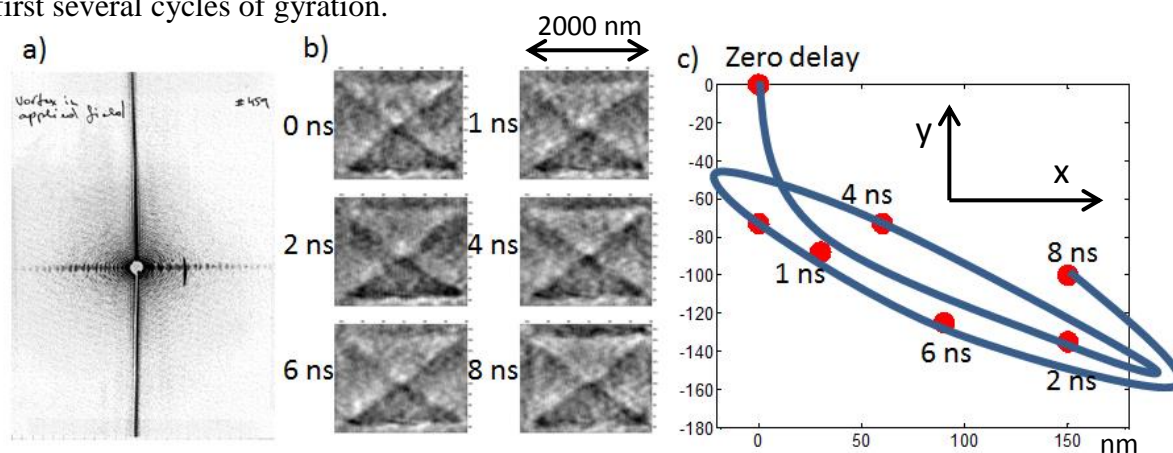


Fig. 4. a) Typical diffraction pattern recorded on CCD. b) Reconstructed images of the domain closure in 2000 x 2000 nm Py square at the different delay times. c) Extracted from the images in (b) the vortex core positions at the different delay times. The blue line is the extrapolated core trajectory of motion.

In total, we imaged 9 points at different time delays (roughly with 1 ns step). Due to time constraints (and a number of technical complications) we did not image delay times with finer resolution. However, even from the given points the cyclic motion of the core allows us to estimate the gyration frequency of the core, which is in the region of 200 MHz (~ 5 ps period), similar to that estimated in the micromagnetic simulations. It should be noted that although the displacement of the core in the vertical direction can be identified with subpixel resolution (~ 25 -30 nm per pixel), the horizontal displacement has a bigger error due to more complex structure of the magnetization around the core in this direction. The optimum resolution in horizontal orientation is also less (by a factor of $\sim\sqrt{2}$) due to tilted sample plane. Our preliminary estimate show that the error in horizontal displacement is ± 20 nm. As stated previously, based on the amount of the displacement from the equilibrium position (~ 100 -150 nm in vertical axis) and the largest diameter of gyration (~ 150 nm), the field produced by the CPW is likely to be in the region of 20-30 Oe. A particular feature that will require further investigation is the shape of the trajectory. It appears highly elliptical, and being skewed horizontally with a principal axis of the ellipsoid tilted with respect to the x-axis. This is in contrast to the micromagnetic simulation where the trajectory is normally

circular at the lower amplitude pulses (in the linear regime). Elliptical trajectory normally implies that the gyration is non-linear. In this case the trajectory is also tilted. We speculate that this can be either due to nonlinearity of the current in the CPW or some effect of interactions from neighboring vortices. This will be further explored in the next round of the proposed measurements.

Identified Issues and the planned improvements.

Firstly, we would like to express our gratitude to the beamline staff for providing the necessary support in preparation and running the experiment. This beamtime was the second (ever) experiment on this newly established beamline, and there was a great amount of effort put by the beamline scientists to make it ready for the start. Nevertheless, given the novelty of the experiment, which was also the first demonstration of the time-resolved measurements using HERALDO, some technical aspects of the measurements took time to get them right.

Beamline alignment. Some of the aspects of that had to be resolved in the beginning of the experiment. This is of course inevitable for any experiment, but first use of our technique led to some additional time spent to get it resolved. Any follow up measurements will account for the difficulties encountered on this occasion.

X-ray beam focusing. Initially the beam focusing was setup to align focal plane with the sample. This however resulted in poor quality of diffraction images. Defocusing of the beam significantly improved the diffraction pattern, however the recorded intensity dropped leading to longer integration time. A possible way to improve the set-up is by moving the pinhole set closer to the samples and thus allowing better coherence while still maintaining more intensive focused beam.

Avalanche diode positioning. In the last days of the experiment the time relation of the ‘pump’ and the ‘probe’ pulse have been lost. It is not clear what led to this effect, but significant time was lost to return the correct time position. In the future experiments the diode should be constantly fixed together with the samples, in case the phase relation needs to be confirmed/identified.

Delay time control. In order to automate the measurements the delay time set by the BCDU8 unit should be controlled from the synoptic of the beamline. This is technically achievable, but due to other constraints we could only use this towards the end of the experiment.

L₃ Iron edge position. Some amount of time was lost due to search for the correct absorption energy position. The optimal value seemed to be found at 710 eV (compared to typical 708).

Crash of exit slit system. Took place during one of the shifts. The problem was related to vacuum pumps, which eventually were restarted directly on the beamline.

Delay time identification on the functional generator. Delays more than 176 ns (greater than the separation between the x-ray pulses) should not be used on the functional generator, as it leads to ‘skipping over’ the following pulse thus mixing the excited and not excited phases.

Generator maximum output. Should be less than 3.8 V (max), as it leads to spontaneous switching off. Some time was lost due to repeating measurements for which this took place.

In principle, the generator has a dual (differential) output, that can be used to make the signal twice as high thus increasing the voltage of the output.